Brazilian Journal of Geophysics

THERMOELASTIC EFFECT IN POROUS MEDIA: DISPERSION AND ATTENUATION ANALYSIS

Izabela B. Noé [ID] [1] , Marcia M. Azeredo [ID] [1] , and Viatcheslav I. Priimenko [ID] [1,2]

ABSTRACT. The theory of thermoelasticity for saturated porous media correlates the heat equation with the poroelastic equations through the coupling between the fields of mechanics deformations and temperature. This theory is widely used in the analysis of high pressure and high temperature reservoirs and other areas of knowledge. We analyze the dispersion and attenuation of the thermoelastic waves depending on the time frequency, thermic, and petrophysical parameters of a medium. Three different poroelastic models coupled with the hyperbolic heat equation are considered: the Biot models, with and without viscous dissipation, and the Biot-JKD model, which involves the dynamic permeability of the rock.

Keywords: thermoelastic coupling; hyperbolic heat equation; Biot/Biot-JKD equations; thermic and petrophysical parameters; dispersion and attenuation effect

RESUMO. A teoria da termoelasticidade para meios porosos saturados correlaciona a equação do calor com as equações poroelásticas através do acoplamento entre os campos de deformações mecânicas e temperatura. Esta teoria é amplamente utilizada na análise de reservatórios de alta pressão e alta temperatura e em outras áreas do conhecimento. Analisamos a dispersão e atenuação das ondas termoelásticas em função da frequência temporal, parâmetros térmicos e petrofísicos de um meio. São considerados três diferentes modelos poroelásticos acoplados à equação do calor hiperbólico: os modelos Biot, com e sem dissipação viscosa, e o modelo Biot-JKD, que envolve a permeabilidade dinâmica da rocha.

Palavras-chave: acoplamento termoelástico; equação de calor hiperbólico; equações Biot/Biot-JKD; parâmetros térmicos e petrofísicos; efeito de dispersão e atenuação

Corresponding author: Viatcheslav I. Priimenko

[1]Universidade Estadual do Norte Fluminense Darcy Ribeiro (UENF), Laboratório de Engenharia e Exploração de Petróleo (LENEP), Campos dos Goytacazes, RJ, Brazil - E-mails: izabelabastos2@gmail.com, marcia578@gmail.com, slava@lenep.uenf.br
[2]Instituto Nacional de Ciência e Tecnologia de Geofísica de Petróleo (INCT-GP/CNPq/MEC), Brazil

INTRODUCTION

The theory of thermoelasticity for a saturated porous medium describes the interaction between deformation and heat exchange. The mathematical equations that model this phenomenon relate the heat equation to Biot's model, describing the coupling between the fields of mechanical deformation and temperature (Noda, 1990; Nield and Bejan, 2006).

The analysis of thermoelastic effects is relevant to study seismic attenuation (Treitel, 1959; Armstrong, 1984), geothermal fields (Carcione *et al.*, 2018), and prospecting for hydrocarbons in general (Fu, 2012, 2017; Jacquey *et al.*, 2015). As conventional hydrocarbon sources decline, the exploration begins to be developed in unexplored or underdeveloped areas. High-pressure and high-temperature reservoirs are increasingly becoming the focus of oil exploration in the search for additional reserves.

Biot (1956a,b) developed the fully dynamic wave propagation theory in a porous medium. He considered a matrix (skeleton or structure) saturated with fluid and predicted the existence of two compression waves (P) and one shear wave (S). The fast P-wave is similar to the compressional wave of the classical elasticity theory. The second compressional wave (also known as Biot's slow wave) is diffusive at low frequencies and has a velocity of propagation lower than the first.

Biot (1962) assumed the continuous mechanical approach applied to measurable optical macroscopic quantities, ignoring the detailed geometric characteristics of the medium microscopic elements (mineral grains, pores, grain contacts). The theory is quite general since it does not assume any factor about the pores and the grain shape and geometry.

Starting with (Biot, 1956c), the theory of thermoelasticity has been well established with time. In this work, Biot explained thermoelasticity by deriving dilatation based on the thermodynamics of an irreversible process and coupling it with elastic deformation. However, the parabolic equation of heat conduction used in this study predicted the infinite velocity for propagating the thermal field. Later, Lord and Shulman (1967) introduced a generalization of thermoelasticity in which a hyperbolic equation of heat conduction with a relaxation time ensured the finite velocity for thermal signals.

The dynamic equations for the theory of thermoelasticity provided four modes of propagation, namely the fast P-wave (elastic wave), the diffusion/slow wave (Biot's slow wave), the diffusion/slow T wave (thermic), and the shear wave (S). For isothermal conditions, the compressional and transversal waves provide the theory of thermoelasticity consistent with the poroelastic waves.

For geophysical exploration, it is interesting to study, in particular, the attenuation and dispersion of waves caused by the presence of viscous fluid in the porous medium. According to Muller *et al.* (2010), when the wave propagates, it generates a pressure gradient in the fluid phase resulting in a relative movement of this to the solid phase. Also, internal friction is caused until the pore pressure is balanced. Due to the action of shear forces, the fluid work on the surface of the pores is transformed into heat, a process called *viscous dissipation*.

For Biot's theory, the fluid flow occurs on the macroscopic scale generating a macroscopic flow, known as global flow, which describes Biot's mechanism. As a result, the attenuation of the global flow is significant only for sonic frequencies (above $100 \, kHz$).

Jonhson *et al.* (1987) published a general expression that described viscous dissipation and established the Biot-JKD model for high frequencies. The model is determined by the dynamic permeability $\kappa(\omega)$ and only one physical parameter is added to the classic Biot's model. The Biot-JKD equations involve fractional derivatives defined by a convolution product in the time domain, which creates difficulties in modeling elastic wave propagation.

This work presents an analysis of the influence of the temporal frequency, relaxation time, thermal conductivity, thermal stress coefficients, porosity, and cementation index (formation factor) on the thermoelastic wave attenuation and dispersion in a thermally conductive saturated porous medium. The mathematical modeling of the problem is formed from three poroelastic models coupled to the hyperbolic heat equation, namely the non-dissipative and dissipative Biot models, and the Biot-JKD model. In this case, the coefficients of the characteristic polynomial of the third order contain complex numbers (except for non-dissipative case), which may lead to incorrect values of the roots calculated by standard formulas. To guarantee the correct values, following Baydoun (2018), we used new analytical expressions to calculate the third-order polynomial roots with complex coefficients. The advantage of this approach is the calculation of the roots of the cubic polynomial as a unified formula using the standardized convention on the square and cubic roots.

BASIC EQUATIONS

Consider an isotropic porous solid thermally conductive and saturated with a fluid. The total stress tensor τ is related to the matrix stress tensor σ and the pore pressure p_f by

$$\tau = \sigma + \alpha(-p_f)\boldsymbol{I}, \tag{1}$$

where α is the Biot parameter that characterizes the bulk coupling between fluid and solid phases and $\boldsymbol{I}$ is the identity matrix. In an isotropic and porous solid saturated by fluid, σ and p_f under isothermal conditions are defined as:

$$\sigma = (\lambda \nabla \cdot \boldsymbol{u})\boldsymbol{I} + \mu(\nabla \boldsymbol{u} + \nabla \boldsymbol{u}^T),$$
$$-p_f = \alpha m \nabla \cdot \boldsymbol{u} + m \nabla \cdot \boldsymbol{w}.$$

Here, λ and μ are the Lamé isothermal coefficients for porous solids, m is an elastic parameter of the isotropic mass coupling of fluid and solid particles (Biot module), $\boldsymbol{w}$ is the vector of the average movement of the fluid in relation to the solid structure defined as $\boldsymbol{w} = \phi(\boldsymbol{U} - \boldsymbol{u})$, where ϕ is the porosity of the solid, while $\boldsymbol{u}$ and $\boldsymbol{U}$ are the absolute displacement vectors in solid and fluid phases, respectively; $(\cdot)^T$ means the transposition.

According to Bear *et al.* (1992) and Levy *et al.* (1995), the thermoelastic constitutive equations considering the porous fluid pressure, the porous matrix stress tensor, and the heat are written as follows:

$$\begin{aligned} \sigma &= (\lambda \nabla \cdot \boldsymbol{u})\boldsymbol{I} + \mu(\nabla \boldsymbol{u} + \nabla \boldsymbol{u}^T) - \beta_s \theta \boldsymbol{I}, \\ -p_f &= \alpha m \nabla \cdot \boldsymbol{u} + m \nabla \cdot \boldsymbol{w} - \beta_f \theta, \\ \psi &= \kappa \nabla \theta - \beta \Theta_0 \left(\tau_0 \partial_t^2 + \partial_t\right)(\boldsymbol{u} + \boldsymbol{w}), \end{aligned} \tag{2}$$

where $\theta = \Theta - \Theta_0$, Θ is the absolute temperature of the porous medium, Θ_0 is a constant reference temperature (temperature of the porous medium in the undisturbed state), κ is the thermal conductivity and τ_0 is the time for relaxation. The thermal stress coefficients for the solid (β_s) and the fluid (β_f) are related by the expression $\beta = \beta_s + \alpha \beta_f$.

Using the constitutive relations (1) and (2), the differential equations for the thermoelastic movement in terms of stresses (τ), fluid pressure (p_f) and relative temperature (θ) can be written as:

$$\begin{aligned} \rho \partial_t^2 \boldsymbol{u} + \rho_f \partial_t^2 \boldsymbol{w} &= \nabla \cdot \tau, \\ \rho_f \partial_t^2 \boldsymbol{u} + \rho_w \partial_t^2 \boldsymbol{w} + g(t) * \partial_t \boldsymbol{w} &= -\nabla p_f, \\ \rho C_e \left(\tau_0 \partial_t^2 + \partial_t\right)\theta &= \nabla \cdot \psi, \end{aligned} \tag{3}$$

where C_e is the specific heat related at constant tension, ρ and ρ_f are the densities of porous aggregate and porous fluid, respectively. The parameter ρ_w is known as the effective density of the fluid that represents the inertial coupling between porous fluid and solid matrix; $\rho_w = \rho_f F$, where F is the formation factor. According to Archie (1942) and Winsauer *et al.* (1952), the parameter F is related to tortuosity a and cementation exponent n as following

$$F = a\phi^{-n}. \tag{4}$$

The term $g * \partial_t \boldsymbol{w}$ characterizes the viscous dissipation induced by the relative movement between the fluid and the elastic skeleton, where the symbol $*$ means the convolution regarding the time variable t. Based on the Fourier transform

$$\hat{h}(\omega) = \int_{\mathbb{R}} h(t)e^{i\omega t}dt, \quad i = \sqrt{-1},$$

function g has the following representation in the time frequency domain ω:

$$\hat{g}(\omega) = \frac{\eta}{\kappa_0} \begin{cases} 0, & \text{non-dissipative Biot model} \\ 1, & \text{dissipative Biot model} \\ \left(1 - i\frac{\omega}{\omega_c}\right)^{1/2}, & \text{Biot-JKD model} \end{cases} \tag{5}$$

with

$$\omega_c = \frac{2\pi f_c}{P}, \quad f_c = \frac{\eta \phi}{2\pi a \kappa_0 \rho_f}, \quad P = \frac{4a\kappa_0}{\phi \Lambda^2}.$$

Here η is the fluid dynamic viscosity, κ_0 is the absolute permeability at zero frequency, f_c is the transition frequency or critical frequency, $a \geq 1$ is tortuosity, and Λ is the typical viscous length. Parameter P is Pride's number (typically $P \approx 1/2$) describing the pores geometry. The limit f_c between the low-frequency range and the high-frequency range is reached when the viscous stresses and inertial effects are similar. For the case of high frequencies, the function $g(t)$ introduces the fractional time derivative displaced in order 1/2, involving a convolution product (Jonhson *et al.*, 1987; Lorenzi and Priimenko, 2014).

THE 1D MODEL

We assume that all physical parameters are constant, i.e., they do not depend on the variables (x, y, z). The displacements will be considered in only one dimension as follows:

$$\boldsymbol{u} = (u(x,t), 0, 0), \quad \boldsymbol{w} = (w(x,t), 0, 0). \tag{6}$$

Substituting Eq. (6) into Eqs. (2) and (3), we obtain the following 1D thermoelastic model:

$$\begin{aligned} \rho \partial_t^2 u + \rho_f \partial_t^2 w &= \partial_x \tau, \\ \rho_f \partial_t^2 u + \rho_w \partial_t^2 w + g(t) * \partial_t w &= -\partial_x p_f, \\ \rho C_e \left(\tau_0 \partial_t^2 + \partial_t\right)\theta &= \partial_x \psi, \end{aligned} \tag{7}$$

where

$$\begin{aligned} \tau &= \left(\lambda + 2\mu + \alpha^2 m\right)\partial_x u + \alpha m \partial_x w - \beta \theta, \\ -p_f &= \alpha m \partial_x u + \alpha m \partial_x w - \beta_f \theta, \\ \psi &= \kappa \partial_x \theta - \beta \Theta_0 \left(\tau_0 \partial_t^2 + \partial_t\right)(u + w). \end{aligned} \tag{8}$$

Remark 1 *In the case $\beta = 0$, the two mechanical waves u and w are decoupled from the thermal wave θ.*

PHASE VELOCITY AND ATTENUATION

Looking for a non-trivial harmonic solution of Eqs. (7) and (8)

$$(u, w, \theta) \backsim \exp\left(i\omega\left(\frac{x}{v} - t\right)\right),$$

we obtain the following dispersion relation

$$c_0 v^6 + c_1 v^4 + c_2 v^2 + c_3 = 0, \qquad (9)$$

where

$$c_0 = \rho C_e \tau_0(\omega)\big(\rho_f \rho'_f - \rho' \rho_w(\omega)\big),$$
$$c_1 = \rho C_e \tau_0(\omega)\Big(H\rho_w(\omega) - (\rho_f \alpha' + \rho'_f \alpha)m + \rho'm\Big)$$
$$-\kappa\big(\rho_f \rho'_f - \rho' \rho_w(\omega)\big) + \beta\beta_f \Theta_0 \tau_0(\omega)\big(\rho' - \rho'_f\big),$$
$$c_2 = -\kappa\Big(H\rho_w(\omega) - (\rho_f \alpha' + \rho'_f \alpha)m + \rho'm)\Big)$$
$$-\rho C_e \tau_0(\omega)(\lambda + 2\mu)m - \beta\beta_f \Theta_0 \tau_0(\omega)\big(H - \alpha'M\big)$$
$$c_3 = (\lambda + 2\mu)\kappa m$$

with

$$H = \lambda + 2\mu + \alpha'\alpha m, \quad \alpha' = \alpha - \frac{\beta}{\beta_f},$$
$$\rho' = \rho - \rho_f \frac{\beta}{\beta_f}, \quad \rho'_f = \rho_f - \rho_w(\omega)\frac{\beta}{\beta_f},$$

and

$$\rho_w(\omega) = \rho_w + \frac{i}{\omega}\hat{g}(\omega), \quad \tau_0(\omega) = \tau_0 + \frac{i}{\omega}. \qquad (10)$$

Equation (9) is cubic in v^2. The roots of this equation can explain the existence of three longitudinal waves in a porous thermoelastic solid. According to Eqs. (5) and (10), the coefficients $\rho_w(\omega)$ (except for non-dissipative case) and $\tau_0(\omega)$ contain complex numbers, which may lead to incorrect values of the roots calculated by standard formulas. To guarantee the correct values, following Baydoun (2018), we used new analytical expressions to calculate the third-order polynomial roots with complex coefficients; see Appendix for details.

The formulas are based on appropriate changes to the variable involving an arbitrary parameter. The advantage of this approach is the calculation of the roots of the cubic polynomial as a unified formula using the standardized convention on the square and cubic roots. On the other hand, the reference formulas for this problem, such as Cardano and Lagrange, provide the roots of the cubic polynomial with incorrect expressions in the case of complex coefficients (Lagrange, 1770; Bourbaki, 1994).

Sharma (2008) defined phase velocity V and attenuation coefficient Q^{-1} by the following formulas

$$V = \frac{\text{Re}^2 v + \text{Im}^2 v}{\text{Re} v}, \quad Q^{-1} = -2\frac{\text{Im} v}{\text{Re} v}. \qquad (11)$$

In Eqs. (11), $\text{Re}\, v$ and $\text{Im}\, v$ denote the real and imaginary parts of the complex velocity v, respectively.

In descending order of phase velocity V, the three waves in a thermoelastic porous medium are identified as P_1 (fast compressional wave), P_2 (slow compressional wave), and T (thermal wave).

NUMERICAL EXAMPLES

Tables 1 and 2 present the elastic and thermal characteristics, respectively, of the homogeneous medium considered in the numerical simulations of this work. These parameters were combined in order to represent a thermally conductive water-saturated sandstone; therefore, they correspond to a synthetic data set.

Table 1. Poroelastic properties

Property	Symbol	Value	Unity
Solid phase density	ρ_s	2644	$Kg\,m^{-3}$
Permeability	κ_0	3.6×10^{-13}	m^2
Porosity	ϕ	0.2	–
Tortuosity	a	2.4	–
Shear module	μ	7.04	GPa
Lamé coefficient	λ	10.6	GPa
Biot module	m	9.70	GPa
Fluid phase density	ρ_f	1000	$Kg\,m^{-3}$
Fluid viscosity	η	1.0×10^{-3}	$Pa\,s$
Viscous length	Λ	5.88×10^{-6}	m
Cementation exponent	n	1.0	–
Biot-Willis parameter	α	0.72	–

Extracted from Blanc (2014)

Table 2. Thermal properties

Property	Symbol	Value	Unity
Specific heat coefficient	C_e	1586.6	$m^2\,s^{-2}\,K^{-1}$
Thermal conductivity	κ	2.75	$W\,m^{-1}\,K^{-1}$
Initial temperature	Θ_0	300	K
Solid phase thermal stress coefficient	β_s	550560	PaK^{-1}
Fluid phase thermal stress coefficient	β_f	667360	PaK^{-1}
Initial relaxation time	τ_0	10^{-6}	s

Extracted from Haibing et al. (2014)

The complexity of this study is characterized by the large number of thermal, elastic, and petrophysical parameters that appear in the coefficients of Eq. (9). This section presents the influence of these parameters on the phase velocity and attenuation of the thermo-poroelastic waves. For this, three different cases are considered: Case I - non-dissipative Biot's model; Case

II - dissipative Biot's model; Case III - the Biot-JKD model.

For a non-dissipative medium, the inertial coupling (or effective density) is $\rho_w(\omega) = \rho_w$, see Eqs. (10). Therefore, for Case I, the attenuation mechanism will be characterized only by $\tau_0(\omega)$.

Effect of frequency

Figures 1 and 2 represent, respectively, the phase velocity and attenuation curves vs. circular frequency (ω) for the two compressional waves P_1 and P_2, and for the thermal wave T.

In the low-frequency range ($\omega < 3 \times 10^4 \, rad/s$), the curves of phase velocities show that P_2- and T-wave are more dispersive than P_1-wave, see Figure 1. The phase velocity of this wave is the same if we consider the cases II (Biot's dissipative model) and III (Biot-JKD model). The P_2-wave has a similar behavior. In the high-frequency range, the dynamic permeability is different from the absolute permeability derived from Darcy's law (Jonhson *et al.*, 1987). As a result, the phase velocities of P_1- and P_2-wave are subtly higher for Case II than for Case III. The phase velocity of the T-wave is the same for the three cases considered in this paper. This means that the viscous dissipation induced by the relative movement between solid and fluid phases does not interfere with the T-wave propagation.

According to Figure 2, the maximum attenuation value of the P_1-wave occurs near the transition frequency, while the peak attenuation of T- and P_2-wave occurs at $\omega = 100 \, rad/s$. We can also observe that the attenuations of P_1- and P_2-wave are almost the same for cases II and III at low frequencies, while at high frequencies, they have a significant difference. It can also be seen that for $5 \times 10^4 \le \omega \le 2 \times 10^6 \, rad/s$, the attenuation of P_1-wave for Case II is more significant than for Case III. On the other hand, when $\omega > 2 \times 10^6 \, rad/s$, the attenuation for Case III is more significant than for Case II. The same behavior occurs for P_2-wave; however, in this case, the effect of dynamic permeability is not so significant. As expected, for the non-dissipative model (Case I), the velocities of P_1- and P_2-wave are constant, and these waves are not attenuated.

Effect of relaxation time

To analyze the relaxation time effect, the value of τ_0 is set to 10^{-6}, 10^{-5} and $10^{-4} \, s$.

In Figures 3 and 4, we use the difference between velocities to explain the influence of the relaxation time variation on the phase velocities of P_1- and P_2-wave. We can only observe a slight difference between waves in the high-frequency domain, which is more obvious for the P_2-wave. The behavior presented characterizes a negligible influence of this term on the responses of P_1- and P_2-wave.

Figure 5(a) shows that in the low-frequency domain, the change in τ_0 has little effect on the phase velocity of the T-wave, and at high frequencies, this effect is more significant. In this case, the shorter the relaxation time, the faster the T-wave. Furthermore, the attenuation curves are more shifted towards the high-frequency domain, see Figure 5(b).

Effect of thermal conductivity

Similar to the effect of relaxation time showed in the previous section, there is a negligible influence of the thermal conductivity κ on the phase velocities of P_1- and P_2-wave. Thus, the results presented are only for T-wave. The relaxation time was defined as $\tau_0 = 10^{-4} \, s$ while the thermal conductivity assumes the values: 2.21, 4.42, and $8.84 \, Wm^{-1}K^{-1}$. Figure 6 shows that the more conductive the medium, the greater its phase velocity. On the other hand, this parameter does not interfere with the T-wave attenuation.

Effect of thermal stress coefficients

To analyze the effect of soil grain thermal stress coefficient β_s, we assume three distinct values: 458800, 917600, and $1376400 \, PaK^{-1}$. Figure 7 shows the phase velocities of waves P_1, P_2, and T as a function of the initial temperature Θ_0. The responses show that the velocities of P_1- and P_2-wave increase when β_s increases. On the other hand, the velocity of the T-wave decreases with an increase of β_s, see Figure 8. Such behavior associated with the T-wave characterizes the greater loss of energy associated with that wave. To analyze the effect of the thermal stress coefficient of fluid β_f, consider the following values: 950600, 1125200, $1299800 \, PaK^{-1}$. Figure 8 shows that the results are similar to β_s-case. The velocities of the P_1- and P_2-wave increase when increasing the thermal stresses β_f and β_s or the initial temperature Θ_0. However, the velocity of the T-wave decreases with the increase of these thermal parameters.

Effect of porosity

To analyze the effect of porosity on the propagation of P_1-, P_2-, and T-wave, we consider the following porosity values: $\phi = 0.2, 0.3, 0.4$. Figures 9 and 10 show, respectively, the porosity effect on phase velocity and attenuation of these waves. We can observe that, in the high-frequency range, when the porosity of the medium increases, the velocities of P_1- and P_2-wave increase too. As a result, these waves become more attenuated. The behavior of the T-wave is the opposite. The lower the porosity value, the higher the phase velocity of T-wave. Besides that, the porosity does not have a significant influence on the T-wave attenuation.
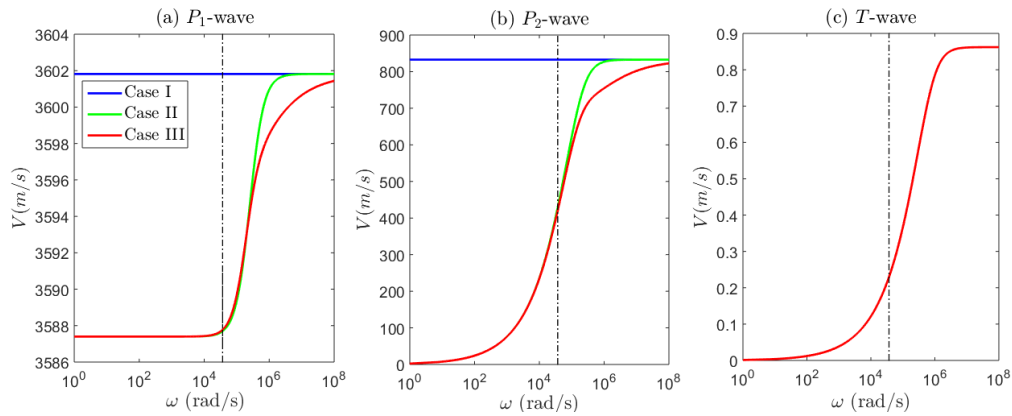
Figure 1. Phase velocity of the thermoelastic waves considering the non-dissipative (Case I) and dissipative (Case II) Biot models, and the Biot-JKD model (Case III)
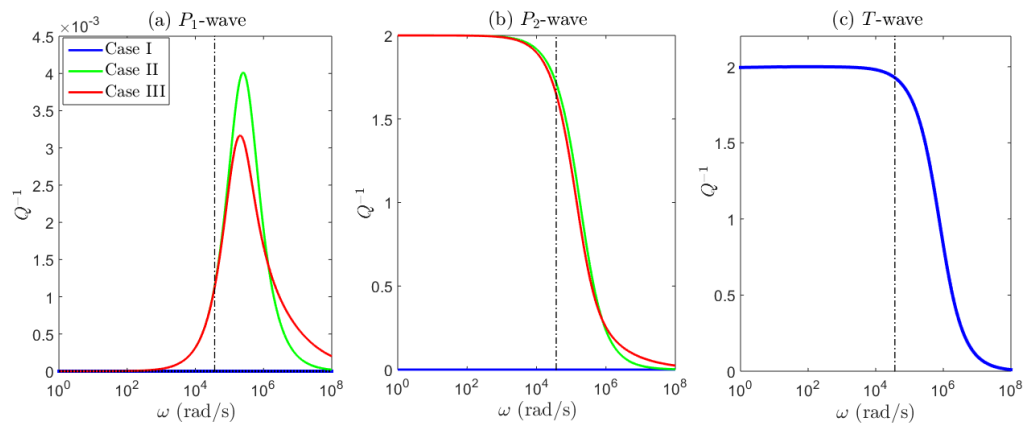

Figure 2. Attenuation of the thermoelastic waves considering the non-dissipative (Case I) and dissipative (Case II) Biot models, and the Biot-JKD model (Case III)
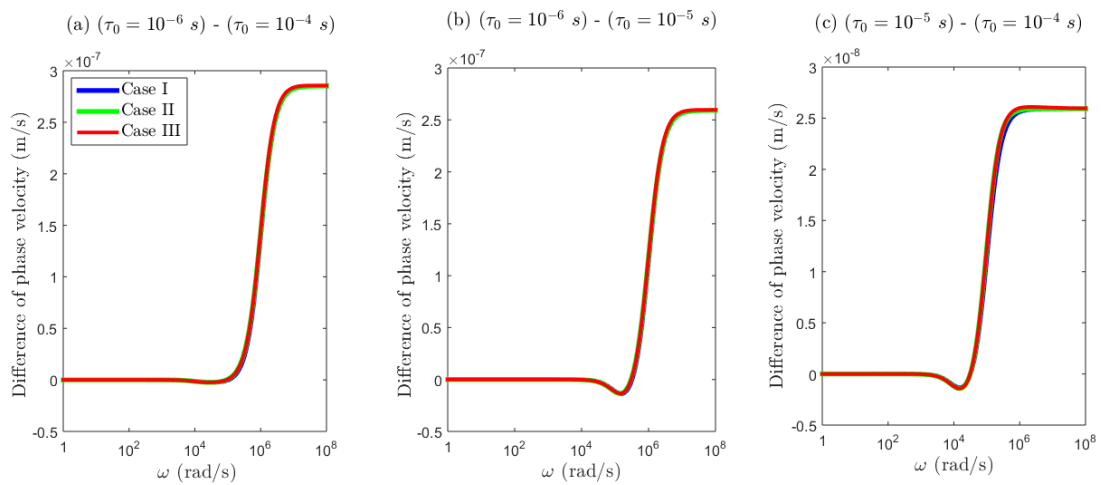

Figure 3. Difference among the phase velocities of P_1-wave considering different relaxation times
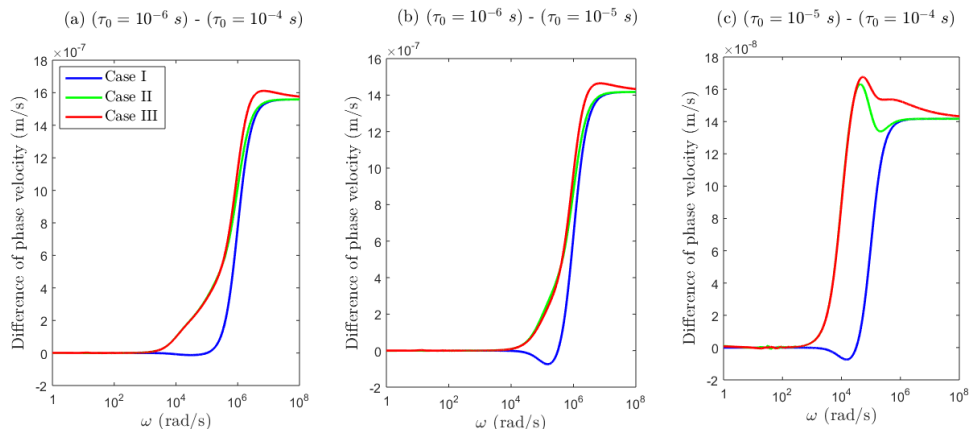
Figure 4. Difference among the phase velocities of P_2-wave considering different relaxation times
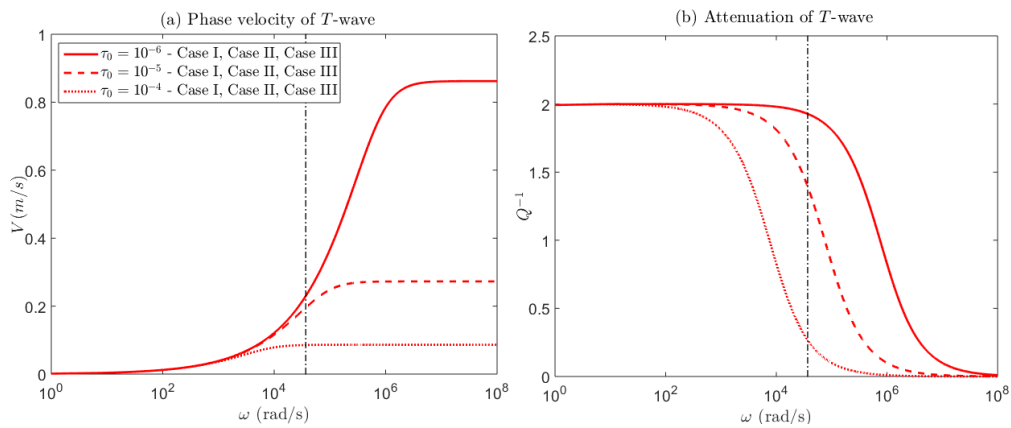
Figure 5. Effect of relaxation time on the phase velocity and attenuation of T-wave
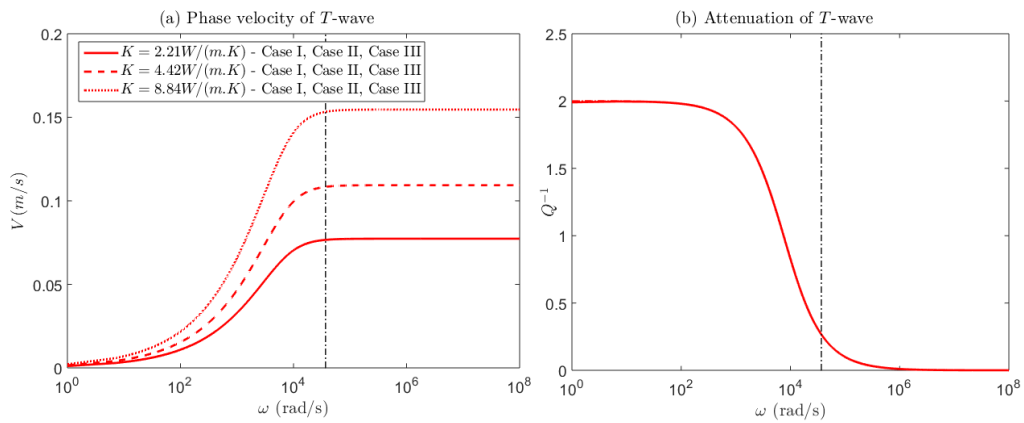
Figure 6. Effect of thermal conductivity on the phase velocity and attenuation of T-wave
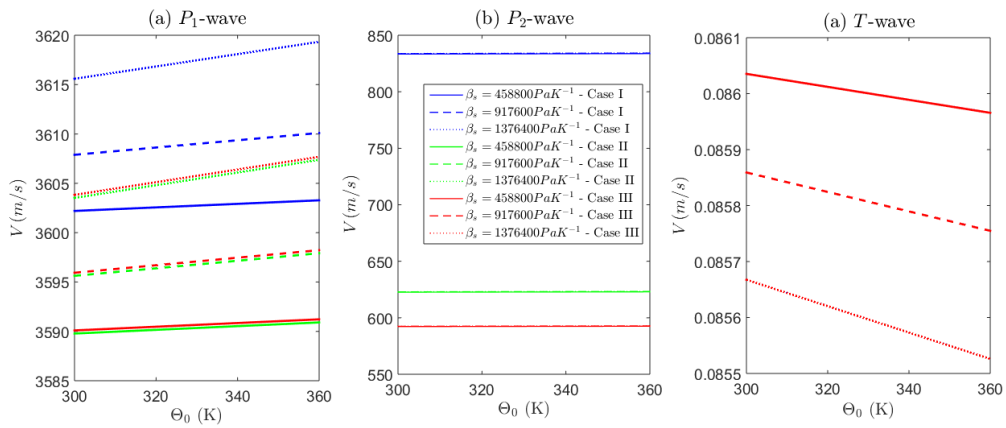
Figure 7. Effect of thermal stress coefficient of solid on the phase velocity
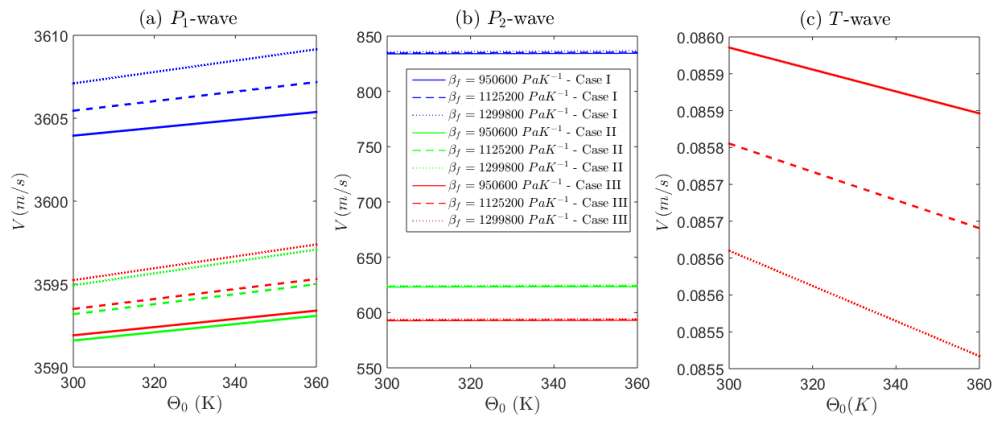
Figure 8. Effect of thermal stress coefficient of fluid on the phase velocity
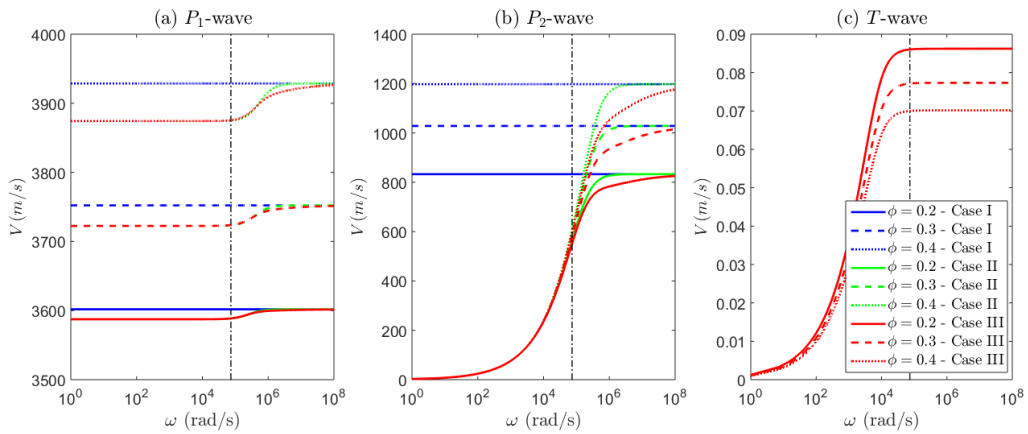
Figure 9. Effect of porosity on the phase velocity
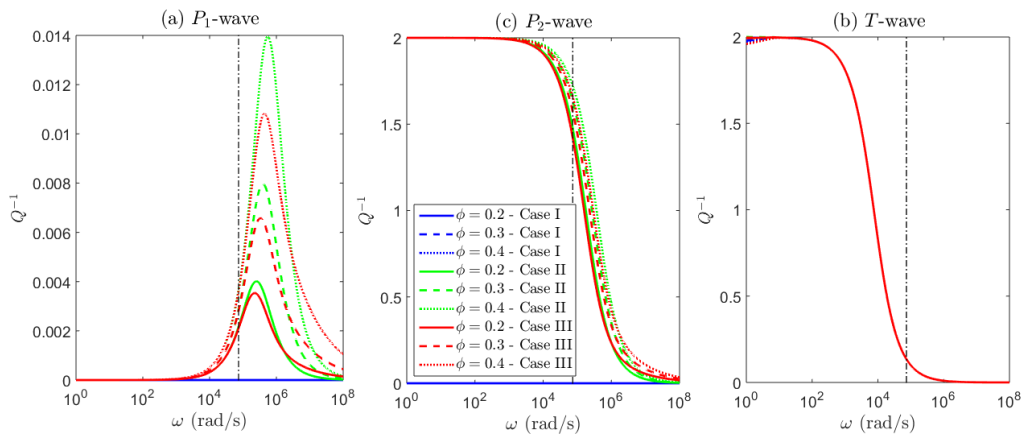
Figure 10. Effect of porosity on the attenuation
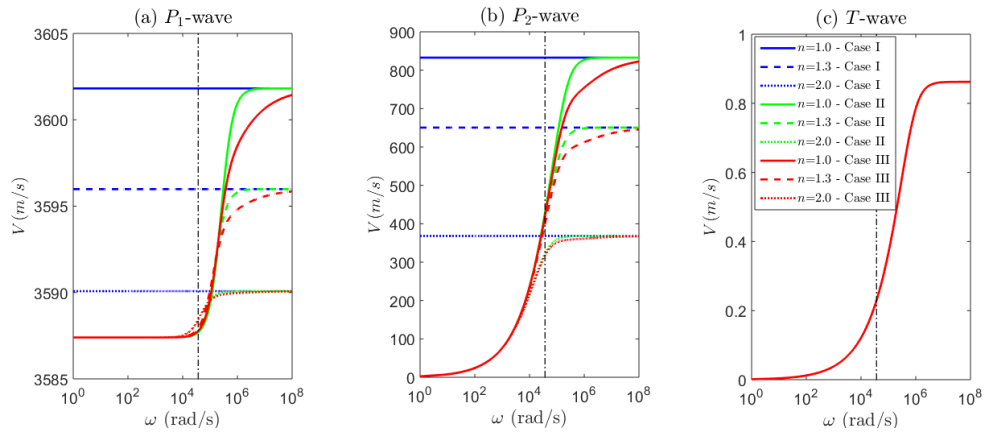
Figure 11. Effect of cementation exponent on the phase velocity
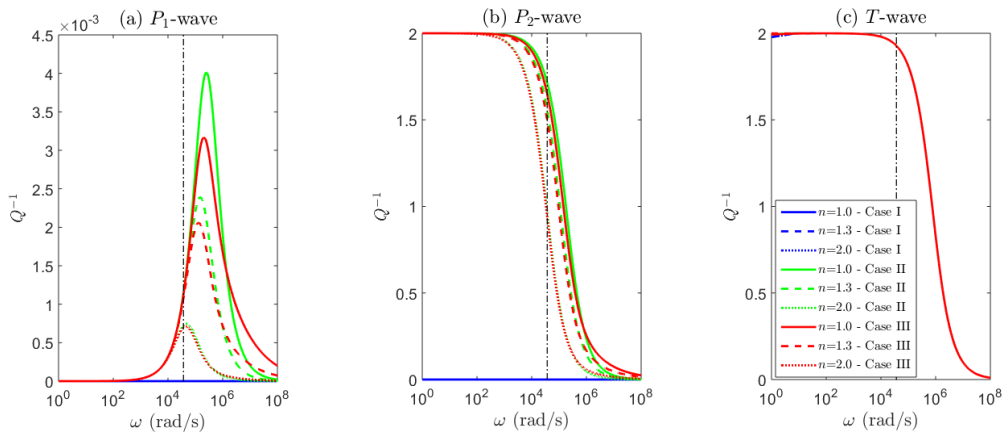
Figure 12. Effect of cementation exponent on the attenuation

Effect of cementation exponent

The studies presented in the previous sections assumed that the cementation exponent n given in the general expression of the formation factor F is equal to 1.

The cementation exponent describes the influence of the pore network on the resistivity since the rock itself is considered non-conductive. If the pore system were to be modeled as a set of parallel capillary tubes, then a cross-section average area of the rocks would give the formation factor (4) with $n = 1$. However, the tortuosity of the rock increases this value, relating the cementation exponent with the permeability of the rock and showing that increasing permeability decreases the cementation exponent. The exponent n has been observed near 1.3 for unconsolidated sands and is believed to increase with cementation. Typical values for consolidated sandstones are $1.8 < n < 2.0$. In carbonate rocks, this parameter has a higher variance due to strong diagenetic affinity and complex pore structure; values from 1.7 to 4.1 have been observed, see (Archie, 1942). This section presents a comparative study of phase velocities and attenuations of thermoelastic waves at different values of n, where $n = 1.0, 1.3, 2.0$; see Figures 11 and 12. At the same time, the other parameters remain unchanged according to Tables 1 and 2. According to Figure 11, when the parameter n increases, the phase velocities of P_1- and P_2-wave decrease, and they start to diverge from each other after the critical frequency. On the other hand, the cementation exponent does not affect the velocity and attenuation of the T-wave; see Figure 12.

CONCLUSION

This work analyzes how the physical parameters affect the phase velocity and attenuation of thermoelastic waves. The processes governed by the hyperbolic heat equation, and the Biot (dissipative and non-dissipative cases) and Biot-JKD equations are considered.

We observe that the frequency range directly influences the phase velocity and attenuation factor behavior, with significant changes close to the critical frequency value. It is also possible to notice that the temperature in the coupled system deformation field becomes more noticeable for the dissipative Biot and Biot-JKD models. The relaxation time significantly changes the thermal wave and meanwhile has a low influence on mechanical waves.

It is also seen that in the case of thermal stress coefficients, mechanical P_1- and P_2-wave and thermal T-wave may have opposite behavior, while the phase velocity of P_1- and P_2-wave increases, the one of T-wave decreases. Also, it is seen how the thermal parameters can significantly affect the behavior of mechanical waves, which is fundamental for understanding the physical processes occurring in a medium with such characteristics.

The thermal effect on wave propagation can vary with changes in the pore characteristics of the porous medium. T-wave has the slowest phase velocity among the three waves obtained. As the relaxation time increases, its phase velocity increases in the low-frequency domain and after the critical frequency, acquiring a stable value at higher frequencies.

It is noticed that together with the porous fluid viscosity, the thermal dissipation might also be a significant cause of elastic wave attenuation in the reservoir rocks and other porous materials.

APPENDIX

Following Baydoun (2018), we represent Eq. (9) as follows:

$$z^3 + bz^2 + cz + d = 0, \quad b, c, d \in \mathbb{C}, \qquad (12)$$

where

$$z = v^2, \quad b = \frac{c_1}{c_0}, \quad c = \frac{c_2}{c_0}, \quad d = \frac{c_3}{c_0}.$$

Introduce the notations:

$$\Delta_l = 2c^3\big(8b^6 + 128b^3d + 36d^3 + 33b^2c^2 - 66bcd\big)$$
$$+ 12b^4c\big(d^2 - 7c^3\big) - b^2c^2d\big(24b^3 + 291d\big)$$
$$+ d^3\big(144bc - 2b^327d\big), \Delta_o = -4b^3d + b^2c^2$$
$$+ 18bcd - 4c^3 - 27d^2, d_o = 4b^4c^2 - 4b^3cd - 14b^2c^3$$
$$+ b^2d^2 + 28bc^2d + c^4 - 12cd^2,$$

and

$$\delta_l = (d - bc)\sqrt{\Delta_o}\big(4b^2c^2 - 4bcd + 2c^3 + d^2\big) + i\frac{\Delta_l}{\sqrt{27}},$$

$$A_1 = -i\frac{2}{\sqrt{3}}\big(4b^3 - 2db^2 - 13bc + 15dc\big) + 2c\sqrt{\Delta_o},$$

$$A_2 = 8b^5c^2 - 8b^4cd - 40b^3c^3 + 2b^3d^2 + 116b^2c^2d$$
$$+ 23bc^4 - 99bcd^2 - 21c^3d + 27d^3 - i\sqrt{3\Delta_o}\big(8b^2c^2$$
$$- 10bcd + c^3 + 3d^2\big).$$

Then the roots of cubic polynomial (12) are:

$$z_m = m\alpha_1 \mathcal{R}_1 + m^2 \alpha_2 \mathcal{R}_2 - \frac{b}{3},$$

$$m \in \left\{ -1, \frac{1 - i\sqrt{3}}{2}, \frac{1 + i\sqrt{3}}{2} \right\}, \qquad (13)$$

where

$$\alpha_1 = \frac{1}{\sqrt{2}} \exp\left\{ i\left[\arg\left(A_1 \sqrt[3]{\delta_l} \right) - \arg\left(-d_o \mathcal{R}_1 \right) \right] \right\},$$

$$\alpha_2 = \frac{1}{\sqrt{2}} \exp\left\{ i\left[\arg\left(A_2 \sqrt[3]{\delta_l^2} \right) - \arg\left(d_o^2 \mathcal{R}_2 \right) \right] \right\}$$

with $\mathcal{R}_1$ and $\mathcal{R}_2$ defined by the following expressions:

$$\mathcal{R}_1 = \frac{1}{3} \sqrt[3]{i\sqrt{27\Delta_o} + 2b^3 - 9bc + 27d},$$

$$\mathcal{R}_2 = \frac{1}{3} \sqrt[3]{i\sqrt{27\Delta_o} - 2b^3 + 9bc - 27d}.$$

Formula (13) is indeed the type of Lagrange, where the square and cubic roots are given by the standard convention, unlike the Cardano and Lagrange formulas that are incorrect with the standard convention. In fact, the difference from previous works is the two terms α_1 and α_2 absent in formulas of Cardano and Lagrange.

REFERENCES

Archie, G. The theoretical resistivity log as an aid in determining some reservoir characteristics. *Petroleum Technology* **1942**, *146*, 54–62.

Armstrong, B. Models for thermoelastic in heterogeneous solids attenuation of waves. *Geophysical Research* **1984**, *49*, 1032–1040.

Baydoun, I. Analytical formula for the roots of the general complex cubic polynomial. France. HAL: hal-01237234v2, 2018.

Bear, J.; Sorek, S.; Ben-Dor, G.; Mazor, G. Displacement waves in saturated thermoelastic porous media. I. Basic equations. *Fluid Dyn. Res.* **1992**, *9*, 155–164.

Biot, M. Theory of propagation of elastic waves in a fluid-saturated porous media. I. Low-frequency range. *J. Acoust. Soc. Am.* **1956a**, *28*, 168–178.

Biot, M. Theory of propagation of elastic waves in a fluid-saturated porous media. II. Higher frequency range. *J. Acoust. Soc. Am.* **1956b**, *28*, 179–191.

Biot, M. Thermoelasticity and irreversible thermodynamics. *J. Appl. Phys.* **1956c**, *27*, 240–253.

Biot, M. Mechanics of deformation and acoustic propagation in porous media. *J. Appl. Phys.* **1962**, *33*, 1254–1264.

Blanc, E. Time-domain numerical modeling of poroelastic waves: the Biot-JKD model with fractional derivatives. PhD thesis, Aix-Marseille University, France, 2014.

Bourbaki, N. *Elements of the History of Mathematics*; Berlin: Springer-Verlag, 1994.

Carcione, J.; Poletto, F.; Farina, B.; Cinzia, B. 3D seismic modeling in geothermal reservoirs with a distribution of steam patch sizes, permeabilities and saturations, including ductility of the rock frame. *Physics of the Earth and Planetary Interiors* **2018**, *279C*, 67–78.

Fu, L. Evaluation of sweet spot and geopressure in Xihu. Sag. Tech. Report CCL2012-SHPS-0018ADM, Key Laboratory of Petroleum Resource Research, Institute of Geology and Geophysics, Chinese Academy of Sciences, 2012.

Fu, L. Deep-Superdeep Oil & Gas Geophysical Exploration. Program report of "111 plan" jointly implemented by the moe and safea, School of Geosciences, China University of Petroleum (East China), 2017.

Haibing, T.; Ganbin, L.; Kanghe, X.; Rongue, Z.; Yuebao, D. Characteristics of wave propagation in the saturated thermoelastic porous medium. *Transport in Porous Media* **2014**, *103*, 47–68.

Jacquey, A.; Cacaea, M.; Biachera, G.; Scheck-Wenderoth, M. Numerical investigation of thermoelastic effects on fault slip tendency during injection and production of geothermal fluids. *Energy Procedia* **2015**, *76*, 311–320.

Jonhson, D.; Koplik, J.; Dashen, R. Theory of dynamic permeability and tortuosity in fluid-saturated porous media. *Journal of Fluid Mechanics* **1987**, *176*, 379–402.

Lagrange, J. Réflexions sur la résolution algébrique des équations. *Nouveaux Mémoires de l'Académie royale des Sciences et Belles-Lettres de Berlin, Oeurves complétes* **1770**, *3*, 205–421.

Levy, A.; Sorek, S.; Ben-Dor, G.; Bear, J. Evolution of the balance equations in saturated thermoelastic porous media following abrupt simultaneous changes in pressure and temperature. *Transport in Porous Media* **1995**, *21*, 241–268.

Lord, H.; Shulman, Y. The generalized dynamical theory of thermoelasticity. *J. Mech. Phys. Solids* **1967**, *15*, 299–309.

Lorenzi, A.; Priimenko, V. Direct problems for poroelastic waves with fractional derivatives. *SIAM. J. Math. Anal.* **2014**, *46*, 1874–1892.

Muller, T.; Gurevich, B.; Lebedev, M. Seismic wave attenuation and dispersion resulting from wave-induced flow in porous rocks - a review. *Geophysics* **2010**, *75*, 75A147–175A164.

Nield, D.; Bejan, A. *Convection in Porous Media*, 3 ed.; Berlin: Springer-Verlag, 2006.

Noda, N. Thermal stress problem in a fluid-filled porous

circular cylinder. *Zeitschrift fur Angewandte Mathematik und Mechanik* **1990**, *70*, 543–549.

Sharma, M. Wave propagation in thermoelastic saturated porous medium. *Journal of Earth System Science* **2008**, *117*, 951–958.

Treitel, S. On the attenuation of small-amplitude plane stress waves in a thermoelastic solid. *Geophysical Research* **1959**, *64*, 661–665.

Winsauer, W.; Shearin, H.; Masson-Jr, P.; Williams, M. Resistivity of Brine-Saturated sands in relation to pore geometry. *AAPG Bulletin* **1952**, *36*, 253–277.

I.N. and **M.A.** Computational implementation, numerical modeling, generation and analysis of the results; **V.P.** Development of mathematical basis, construction of the workflow and analysis of the results.